Single optical surface imaging designs with unconstrained object to image mapping with non-rotational symmetry

Jiayao Liu*[a], Juan C. Miñano [ab], Pablo Benítez[ab]
[a]Universidad Politécnica de Madrid, Cedint, Campus Montegancedo, Pozuelo, 28223 Madrid, Spain;
[b]LPI, 2400 Lincoln Avenue, Altadena, CA 91001, USA

ABSTRACT

In this work, novel imaging designs with a single freeform optical surface (either refractive or reflective) are presented. In these designs, not only the mapping is obtained in the design process, but also the shape of the object is found. In the examples considered, the image is virtual and located at infinity and is seen from known pupil, which can emulate a human eye.

In the first introductory part, 2D designs and 3D designs by rotation using the differential equation method for the limit case of small pupil have been reviewed. Furthermore, the differential equation method is used to provide the freedom to control the tangential rays and sagittal rays simultaneously.

In the second part, according to the study of astigmatism of different types of design with rotational symmetry, the differential equation method for 3D rotational design without astigmatism (at the small pupil limit) on a curved object surface has been extended to 3D freeform design. The result of this extended method has been proved to coincide with the former 3D design by rotation which is a special case of 3D freeform design. Finally, the initial condition has been used as an additional freedom to control the shape of the object surface. As a result, a reflective design with a much flatter object surface has been obtained.

Keywords: Head-mounted displays, imaging, anastigmatic, differential geometry, freeform

1. INTRODUCTION

The first graphics-driven head-mounted display (HMD) was developed by Ivan Sutherland in the 1960s[1]. This display system is supposed to be worn on the human head, providing three-dimensional interactive displays while not limiting not only the free motion of the head, but also the potential body movement. Considering the fact that the humans have not evolved to wear heavy devices on the head, the lightweight and ergonomics have been the important criterion for the design of HMD[2].

The human eye sees the modulated light source through an optical system. There are already a few display technologies like Active-Matrix Liquid-Crystal-Displays (AM-LCDs), Ferroelectric Liquid Crystal on Silicon (FLCOS), Organic Light Emitting Displays (OLED) and etc. which contribute in developing micro displays with high resolution and uniform luminance. A simple optical system is also needed to achieve the goal of lightweight and ergonomic.

A design of a single optical surface that forms the mapping from the object, which refers to the screen of the micro display, to the image, which refers to the retina of the human eye, through a known pupil, which emulates the pupil of the eye, is presented in this paper. An average MTF of 67.5% at 23 cyc/mm and an average spot size of 0.01918 mm have been achieved.

2. 2D DESIGN AND 3D ROTATIONAL DESIGNS

The design procedure explained in this part is 2D designs and 3D designs obtained by the rotation of 2D ones. Due to the reversibility of optical path, the design can be considered as a design of a single optical surface forming a mapping of the rays from the source, which was the pupil, with angle θ respected to the optical axis to the image plane, which was the object, at the point $x(\theta)$. The sketch map of the refractive and reflective design is shown in Fig. 1.

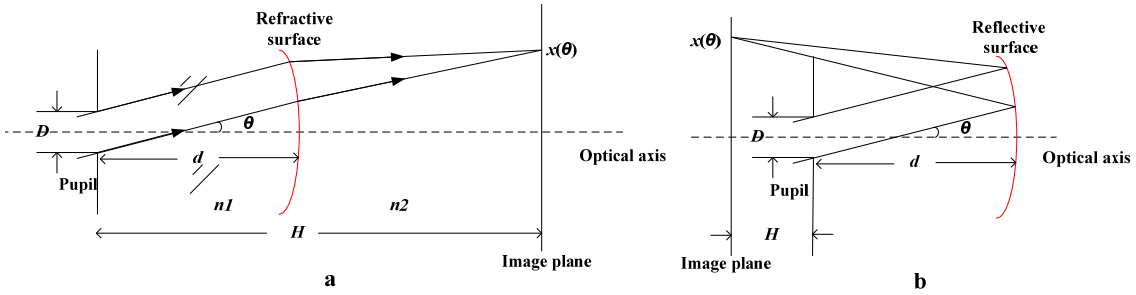

Figure 1. Sketch map of the refractive design (a) and the reflective design (b)

2.1 2D designs

The differential equation method depends on the local properties of the wave fronts and the surfaces, which can be expressed in differential form. Thus the generalized ray tracing can be expressed by concepts of differential geometry. Generally, a wave front travels from one media to another through a certain interface, will change to another wave front. In two dimensions, this propagation can be expressed by following equations:

$$\begin{cases} \dfrac{n_2 \cos^2 \theta_2}{\rho_2} = \dfrac{n_1 \cos^2 \theta_1}{\rho_1} + \dfrac{\gamma}{\rho_s} \\ \gamma = n_2 \cos\theta_2 - n_1 \cos\theta_1 \end{cases} \tag{1}$$

where n denotes refractive index, ρ denotes the radius of curvature[3].

Considering that the wave front from the pupil is in fact a plane, the radius of curvature is infinity. With the prescribed image surface, the radius of curvature of the wave front after the optical surface can be described by the radius of curvature of the optical surface. Under the polar coordinate $(r(\theta), \theta)$, the radius of curvature and the normal of the optical surface can be expressed by r, θ, $dr/d\theta$ and $d^2r/d\theta^2$. Thus the equation (1) has converted to a second order ordinary differential equation. By solving the equation, an optical surface and its mapping have been obtained. The above-mentioned equation is applicable for both the reflective and refractive design.

The refractive design example based on this method has been compared with the designs of same dimension from other two design methods: Compound Cartesian Oval[4] and SMS 2D[4, 5, 6, 7]. When the pupil is small enough to be considered as a point source, all the three methods have provided very similar optical surface, object to image mapping and image quality. But when the pupil has a certain size that cannot be ignored, the existing tiny difference will lead to great difference in imaging. The refractive example used here consists of a round pupil with the size of 1 unit in diameter, the optical surface 5 units from the pupil and the image plane 10 units from the pupil on the optical axis. The comparison of angular RMS[8, 9] of the three methods is shown in Fig. 2 to provide a more direct and vivid understanding of the difference between the design methods.

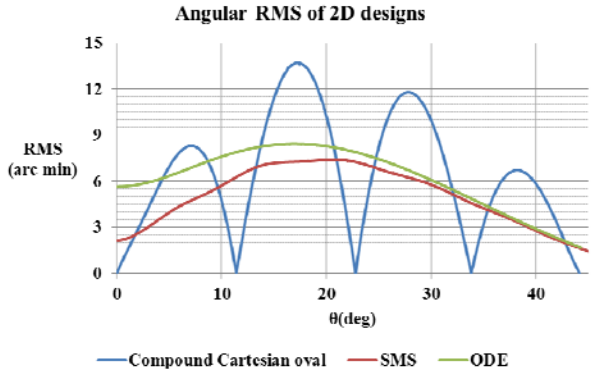

Figure 2. Angular RMS of the three 2D design methods

The compound Cartesian oval works perfectly when the incident angle equals to the designing angle, but contains the highest RMS when far away from them, thus the curve shows an oscillatory shape. The SMS method considers two edge rays from the pupil for the imaging point, which has smoothed and improved the performance. The ODE method is based on the local properties of an infinitesimal part of the surfaces, which only deals with an infinitesimal bundle of rays, a single ray in other words, from point sources, thus provides little bit worse results than SMS method.

2.2 3D rotational designs

A 3D design can be obtained by rotating the former 2D designs on the optical axis. When doing this, not only the tangential condition, but also the sagittal condition has to be taken into account. Though SMS method has provided the best angular RMS result in 2D designs, when extended to 3D rotational cases, in the tangential plane, the rays follow the same condition in 2D and focus on the correspondent position on the rotated image plane, in the sagittal plane, due to the lack of freedom in 2D design, we cannot ensure that the sagittal rays focus on the same image plane.

Take the 2D ODE design for example, the design was in two dimensions, which refers to the tangential plane in three dimensions, and the tangential rays can focus on the prescribed image plane (Fig. 3(a)). The sagittal plane is perpendicular to the design plane and the curvature of the optical surface in this direction is different from that of the tangential direction, which makes the sagittal rays focus on an image plane other than the designed one (Fig. 3(b)).

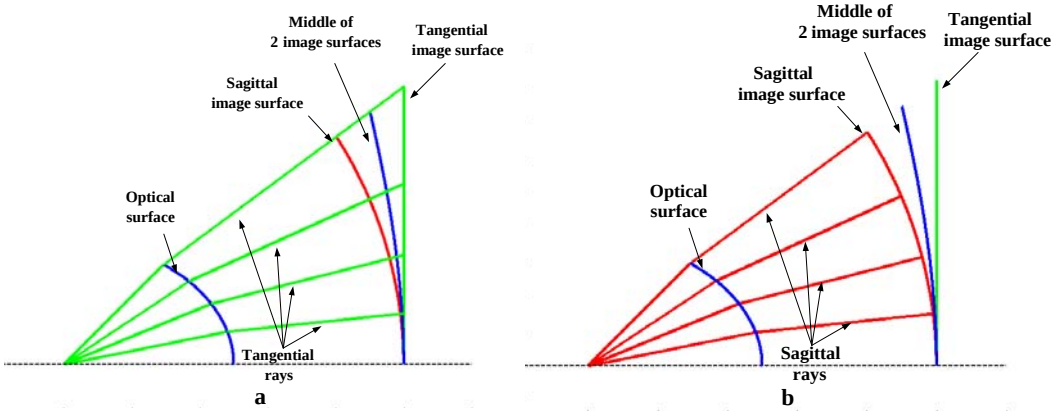

Figure 3. In 3D rotational design, tangential rays (a) and sagittal rays (b) don't focus on the same place

In 3 dimensions, considering the tangential and sagittal direction simultaneously, the generalized ray tracing equation has become to:

$$\begin{cases} \dfrac{n_2\cos^2\theta_2}{\rho_{q2}} = \dfrac{n_1\cos^2\theta_1}{\rho_{q1}} + \dfrac{\gamma}{\rho_{qs}} \\ \dfrac{n_2}{\rho_{p2}} = \dfrac{n_1}{\rho_{p1}} + \dfrac{\gamma}{\rho_{ps}} \\ \gamma = n_2\cos\theta_2 - n_1\cos\theta_1 \end{cases} \tag{2}$$

where q denotes the tangential direction and p denotes the sagittal direction.

The equation (2) gives us more freedom of design. That is to say, we can control both the tangential and the sagittal rays at the same time in the design. For instance, a design makes the middle plane between the tangential image plane and the sagittal image plane a flat plane (see Fig. 4) in order to get a uniform astigmatism. Or a design makes the tangential image plane and the sagittal image plane the same in order to get anastigmatic design (see Fig. 5).

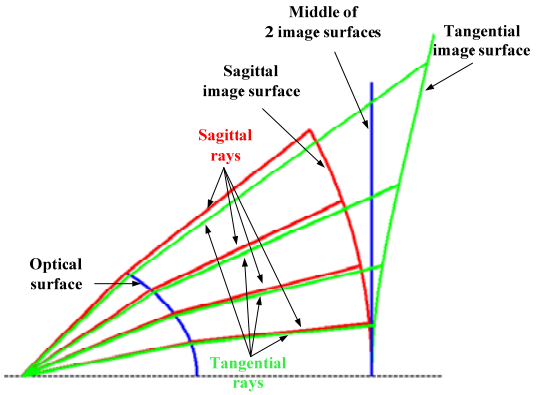

Figure 4. 3D rotational design with the flat image plane of uniform astigmatism

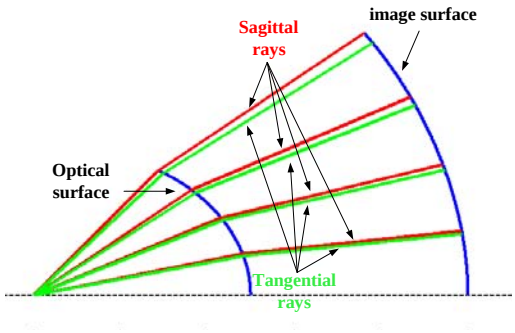

Figure 5. 3D rotational anastigmatic design

A round pupil with the size of 5mm in diameter has been chosen to emulate the human eye; the optical surface and the image plane are 25mm and 50mm away respectively from the pupil on the optical axis for the refractive design; the optical surface and the image plane are 25mm and -10mm away respectively from the pupil on the optical axis for the reflective design. The angular RMS of 2D ODE design, flat image plane of uniform astigmatism design and anastigmatic design has been compared (see Fig. 6).

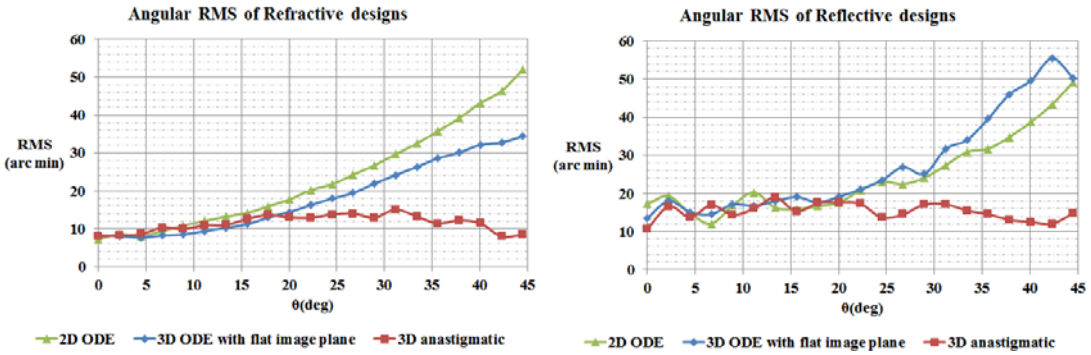

Figure 6. Angular RMS of the 2D ODE design, flat image plane of uniform astigmatism design and anastigmatic design

From the comparison of the result, we can deduce that the 3D differential equation is a useful method for the design of small astigmatism, especially for large angles.

3. 3D FREEFORM DESIGN

In real applications, a flat image plane is always much more needed. We have applied equation (2) to the 3D freeform anastigmatic design. Since 3D freeform design is much more difficult than that of 2D and 3D rotational, here we only focus on reflective designs, which doesn't concern the change of refractive index.

In three dimensions, a surface can be expressed by equation (3), the two solutions of which are two principle curvatures of the surface.

$$\left(EG - F^2\right)\lambda^2 - \left(EN + GL - 2FM\right)\lambda + LN - M^2 = 0 \tag{3}$$

Since the wave front from the pupil is a plane wave and the wave front after the optical surface is spherical, so that both the tangential and sagittal rays can focus on the same position, we can deduce that the two radius of curvature of the surface in equation (2) are radius of principle curvatures, which are solutions of equation (3) with F=M=0 and fulfill the equation (4).

$$\frac{\rho_{ps}}{\rho_{qs}} = \cos^2\theta_o \tag{4}$$

In spherical coordinates, the above equations brought us a partial differential equation (5)

$$a\frac{\partial^2 r}{\partial\theta^2} + b\frac{\partial^2 r}{\partial\theta\partial\varphi} + c\frac{\partial^2 r}{\partial\varphi^2} = e \tag{5}$$

where a, b, c, e are functions of r, θ, φ, p, q, where $p=\partial r/\partial\theta$, $q=\partial r/\partial\varphi$.

This is a typical second order hyperbolic partial differential equation. Assuming that the surface and the image curves of 3D rotational anastigmatic design are the symmetrical axis of the optical surface and the image surface respectively, we then have enough initial conditions of r, θ, φ, p, q to find the numerical solution[10].

We have compared the numerical solution with the 3D rotational anastigmatic design to test the numerical solution by the chosen algorithm (see Fig. 7).

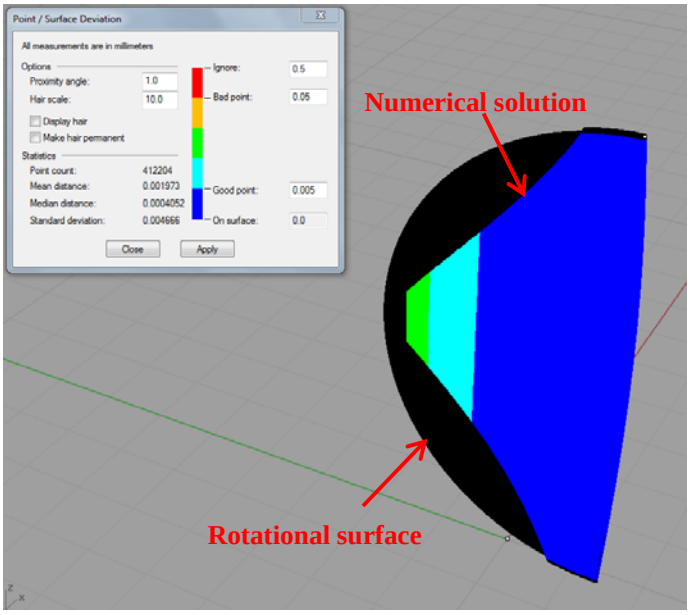

Figure 7. Comparison between 3D rotational anastigmatic design and the numerical solution

The values of the deviation between the two designs shown in Figure 7, which are in mm, are very small indicating that the 3D rotational anastigmatic design coincides with the solutions of 3D freeform anastigmatic design. This theoretically proves the correctness of the numerical algorithm.

Now we can free the sagittal elements from the rotational restriction by assuming that the symmetrical axis are 2D ODE design, in which the axis of the image surface is a straight line instead of the former curve of 3D rotational anastigmatic design. We then have another initial condition of r, θ, φ, p, q. The numerical solution leads to a much flatter image surface (see Fig. 8).

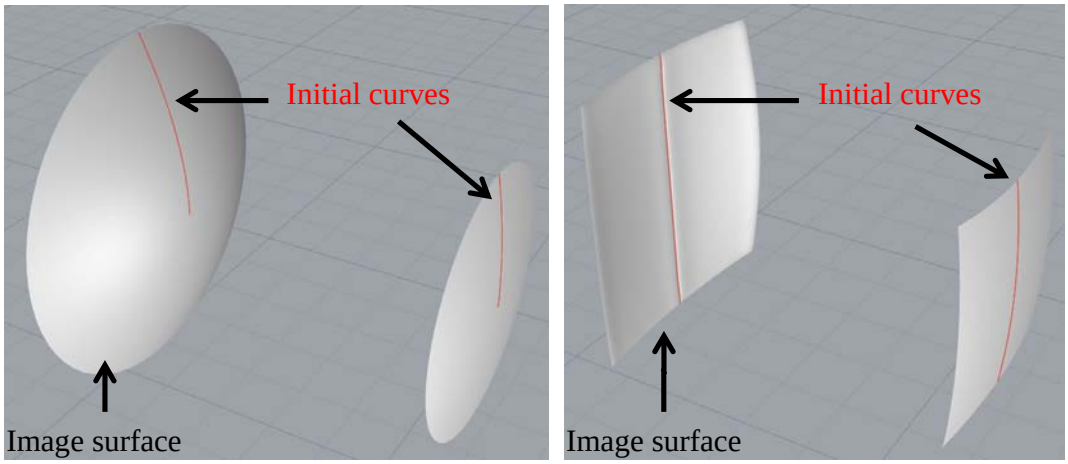

a b

Figure 8. 3D anastigmatic design with very curved image surface (a) and much flatter image surface (b)

The max deviation between the radius of tangential and sagittal outgoing wave fronts is less than 0.1% over the average value, indicating that this numerical solution represents an anastigmatic design.

4. 3D FREEFORM DESIGN EXAMPLE

As an optical design example, a single optical surface with a flat image plane approximation with multiple fields is optimized. The example system has a >15 mm eye clearance, 3mm pupil, 24° diagonal full field of view (9.56° x semi-field and 7.2° y semi-field), and 11.2° mirror tilt angle. The distance from the pupil to the mirror vertex is 17.7 mm. Distance from the mirror vertex to the image plane is around 13 mm so that the micro display won't be too close to the human eye. The image plane has a rectangular aperture with a size of 4.8mm and 3.6 mm in the x and y dimensions respectively. The whole system is set to ensure that there are no blocks on the ray path between the pupil and the mirror (see Fig. 9).

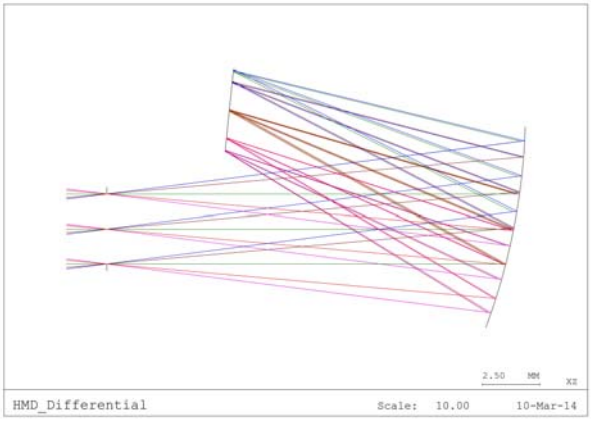

Figure 9. Optical layout of the system

Modulation Transfer Function (MTF) is evaluated for 17 fields (see Fig. 10) and an average value of 67.5% at 23 cyc/mm has been achieved. An average spot size of 0.01918 mm with maximum of 0.02288 mm has been achieved.

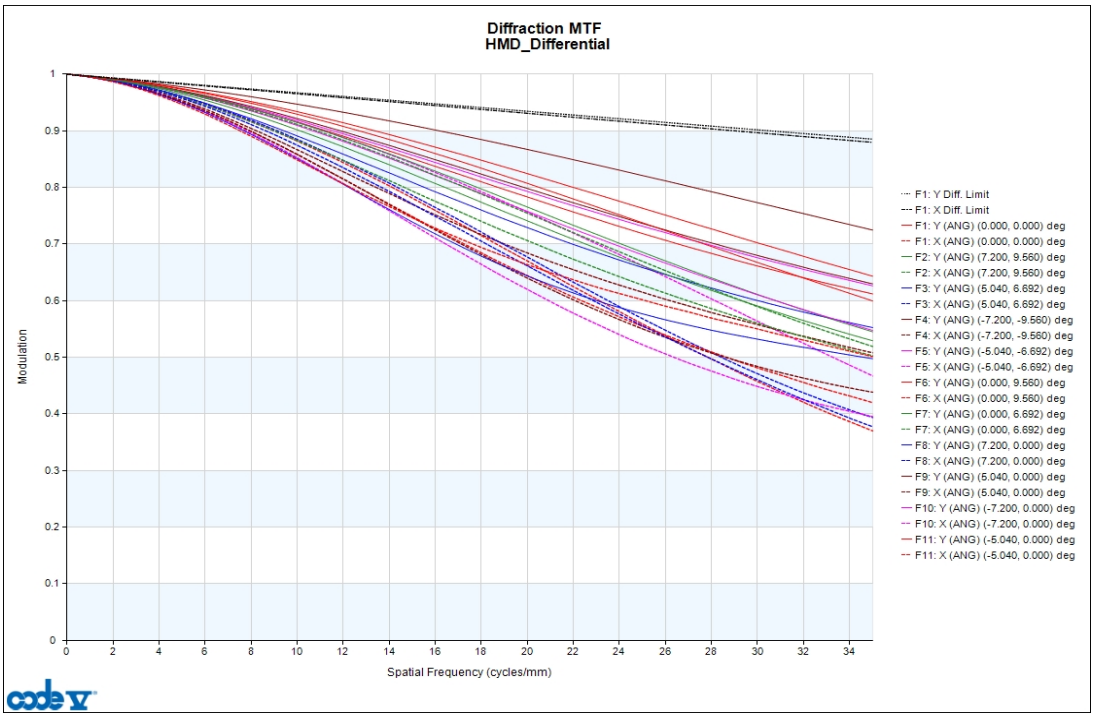

Figure 10. MTF evaluated on 17 fields (considering axisymmetric, 11 fields are plotted)

5. CONCLUSION

We have presented the differential equation method for single optical surface imaging design with object to image mapping, which can provide more freedom for the design and the best result in 3D rotational designs among existing design methods presented here. The successful extension to 3D freeform designs has shown a very good result for applications.

6. ACKNOWLEDGMENTS

Authors thank the European Commission (SMETHODS: FP7-ICT-2009-7 Grant Agreement No. 288526, NGCPV: FP7-ENERGY.2011.1.1 Grant Agreement No. 283798), the Spanish Ministries (ENGINEERING METAMATERIALS: CSD2008-00066, SEM: TSI-020302-2010-65 SUPERRESOLUCION: TEC2011-24019, SIGMAMODULOS: IPT-2011-1441-920000, PMEL: IPT-2011-1212-920000), and UPM (Q090935C59) for the support given to the research activity of the UPM-Optics Engineering Group, making the present work possible.

REFERENCES

[1] Sutherland, I. E., "A head-mounted three-dimensional display," Proceedings of fall joint computer conference, part I (AFIPS '68 (Fall, part I)), 757-764 (1968).
[2] J.P. Rolland and H. Hua, "Head-mounted display systems," Encyclopedia of Optical Engineering, Ronald G. Driggers, Craig Hoffman, Ronald Driggers, Taylor & Francis (2003).
[3] Orestes N. Stavroudis, [The Mathematics of Geometrical and Physical Optics: The k-function and its Ramifications], Wiley-VCH, Berlin, 97-114 (2006).

[4] Jiayao Liu, Juan C. Miñano, Pablo Benítez, Lin Wang, “Single optical surface imaging designs with unconstrained object to image mapping,” Proc. SPIE 8550, Optical Systems Design 2012, 855011 (December 18, 2012); doi:10.1117/12.981210.
[5] Juan C. Miñano, Pablo Benítez, Wang Lin, Fernando Muñoz, José Infante, Asunción Santamaría, "Overview of the SMS design method applied to imaging optics," Proc. SPIE 7429, Novel Optical Systems Design and Optimization XII, 74290C (2009).
[6] R. Winston, J. C. Miñano, P. Benítez, [Nonimaging Optics], Academic Press, New York, 181-217 (2005).
[7] J. Chaves, [Introduction to Nonimaging Optics], CRC Press, Boca Raton, FL, 271-324 (2008).
[8] Wang Lin, Pablo Benítez, J. C. Miñano, José Infante, Guillermo Biot, "Advances in the SMS design method for imaging optics, " Proc. SPIE 8167, Optical Design and Engineering IV, 81670M (2011).
[9] Wang Lin, Pablo Benítez, J. C. Miñano, José Infante, Guillermo Biot, "Progress in the SMS design method for imaging optics, " Proc. SPIE 8128, Current Developments in Lens Design and Optical Engineering XII; and Advances in Thin Film Coatings VII, 81280F (2011).
[10] E.H. Twizell, "The numerical solution of second order hyperbolic partial differential equations with unequally spaced initial conditions," The Computer Journal, 18, 252-257 (1975).